Translational Oncology 21 (2022) 101425

Contents lists available at ScienceDirect

Translational Oncology

journal homepage: www.elsevier.com/locate/tranon

Original Research

Low doses of niclosamide and quinacrine combination yields synergistic effect in melanoma via activating autophagy-mediated p53-dependent apoptosis

Xuan Zheng [a,b,1], Jianyun Zhang [c,1], Shuangting Li [d,1], Xiaolei Gao [a,b], Yixin Zhang [a,b], Meng Wang [a], Liying Dong [a,b], Liangjie Sun [a,b], Na Zhao [e,f], Zeyun Ma [g,*], Chong Ding [a,*], Yixiang Wang [a,b,**]

[a] Central Laboratory, Peking University School and Hospital of Stomatology, No.22, Zhongguancun Avenue South, Haidian District, Beijing 100081, China
[b] Department of Oral and Maxillofacial Surgery, Peking University School and Hospital of Stomatology, No.22, Zhongguancun Avenue South, Haidian District, Beijing 100081, China
[c] Department of Oral Pathology, Peking University School and Hospital of Stomatology, No.22, Zhongguancun Avenue South, Haidian District, Beijing 100081, China
[d] Shanxi Province Key Laboratory of Oral Diseases Prevention and New Materials, Shanxi Medical University School and Hospital of Stomatology, Taiyuan 030001, China
[e] Department of Restorative Dentistry and Biomaterials Sciences, Harvard School of Dental Medicine, Boston, MA, USA
[f] Shanghai Stomatological Hospital, Fudan University, No.356, Beijing Road East, Shanghai, China
[g] Department of VIP Service, Peking University School and Hospital of Stomatology, No.22, Zhongguancun Avenue South, Haidian District, Beijing 100081, China

ARTICLE INFO

Keywords:
Melanoma
Niclosamide
Quinacrine
Autophagy
Apoptosis

ABSTRACT

Malignant melanoma is a highly aggressive, malignant, and drug-resistant tumor. It lacks an efficient treatment approach. In this study, we developed a novel anti-melanoma strategy by using anti-tapeworm drug niclosamide and anti-malarial drug quinacrine, and investigated the molecular mechanism by *in vitro* and *in vivo* assays. Meanwhile, other types of tumor cells, immortalized epithelial cells and bone marrow mesenchymal stem cells were used to evaluate the universal role of anti-cancer and safety of the strategy. The results showed, briefly, an exposure to niclosamide and quinacrine led to an increased apoptosis-related protein p53, cleaved caspase-3 and cleaved PARP and autophagy-related protein LC3B expression, and a decreased expression of autophagy-related protein p62, finally leading to cell apoptosis and autophage. After inhibiting autophagy by Baf-A1, flow cytometry and western blot showed that the expression of apoptosis-related proteins was down-regulated and the number of apoptotic cells decreased. Subsequently, in the siRNA-mediated p53 knockdown cells, the expression of apoptosis-related proteins and the number of apoptotic cells were also reduced, while the expression of autophagy-related proteins including LC3B, p62 did not change significantly. To sum up, we developed a new, safe strategy for melanoma treatment by using low doses of niclosamide and quinacrine to treat melanoma; and found a novel mechanism by which the combination application of low doses of niclosamide and quinacrine exerts an efficient anti-melanoma effect through activation of autophagy-mediated p53-dependent apoptosis. The novel strategy was verified to exert a universal anti-cancer role in other types of cancer.

Introduction

Malignant melanoma, a highly aggressive drug-resistant tumor, is formed by the deterioration of melanocytes [1]. Although, compared with other common malignant tumors, its incidence is relatively low, accounting for about 2% of all malignant tumors, but it is one of the most malignant tumors. According to statistics, the incidence of melanoma only accounts for 10% of skin cancer, but the mortality rate accounts for

* Corresponding authors.
** Corresponding author at: Central Laboratory, Peking University School and Hospital of Stomatology, No.22, Zhongguancun Avenue South, Haidian District, Beijing 100081, China.
E-mail addresses: kqmzy101@sina.com (Z. Ma), idtbbsb@163.com (C. Ding), kqwangyx@bjmu.edu.cn (Y. Wang).
[1] These author contributed equally to this work.

https://doi.org/10.1016/j.tranon.2022.101425
Received 4 April 2022; Accepted 7 April 2022

nearly 80% of skin cancer-related deaths [2]. Melanoma incidence is getting higher in recent years. There were approximately 100,000 new cases in 2019, which causes a huge burden on the global public health burden [3].

Although new breakthroughs have been made in pathogenesis and treatment methods in past decade years, the 5-year survival rate of patients with metastatic melanoma is always less than 15% due to drug resistance and recurrence. The median survival time of melanoma patients is no more than 12 mon [4]. Therefore, in order to improve the prognosis of the patients of malignant melanoma, it is urgent to explore new and effective drugs and treatment strategies.

Compared to the high economic and time cost of new drug development, drug repurposing has some obvious advantages, such as the definite biological safety, less economy burden and short process [5].

Niclosamide (N) is a widely used oral anti-helminthic drug and have gained FDA approvement for about 40 years [6]. In recent years, it is discovered to have a therapeutic effect on various diseases, ranging from cancer (including melanoma), metabolic syndrome and many types of infections [7]. Among them, the anti-cancer effect has attracted much more attention. Previous studies have found that niclosamide exerts its inhibitory effect by affecting multiple pathways [8], including Wnt/β-catenin [9], mTORC1 [10], STAT3 [11], NF-κB [12] and Notch1 pathways [13], thus inhibits cancer cells proliferation and induces cell death.

Quinacrine (QC) was discovered in 1932 by Schulemann and has been used for the treatment of malaria since 1978 [14]. In the past decades, researchers have found that the antimalarial drug quinacrine is a promising drug in cancer (including melanoma) treatment due to its advantages in targeting multiple pathways with slight side effects such as headache, dizziness, or gastrointestinal symptoms [15]. Quinacrine inhibits the arachidonic acid pathway through a direct inhibitory effect on the activity of the PLA2 enzyme that is of great importance for eicosanoids production [16,17], and reduces production of prostaglandin E2 [15]. Prostaglandin E2 is responsible for inducing pro-inflammatory response and inhibiting tumorigenesis consequently [18]. In addition, quinacrine has multiple anti-cancer properties, for examples, quinacrine increases receptor binding of TRAIL and p53 expression, traps facilitate chromatin transcription complex, just inhibiting DNA damage repair as well as cause cell cycle arresting in S phase, thus activate apoptosis of cancer cell [19,20]. Quinacrine promotes autophagic vesicles generation through LCB3 and hinders the selective autophagy receptor of p62 and as a result, activates autophagic cell death [21,22]. However, the effects of these two drugs combination on melanoma were still largely unknown.

Cell death has been observed in cancers for a long time, it was once believed there were only two forms of cell death processes, apoptosis (also known as programmed cell death) and necrosis (uncontrolled cell death) [23]. In recent twenty years, other forms of cell death have been discovered, such as pyroptosis [24], necroptosis [25], entosis [26], ferroptosis [27], autophagy [28] and alkaliptosis [29]. Among them, apoptosis and autophagy were paid more attention owing to the important roles in cancer development, progression and treatment sequelae.

Our research group has been intensively researching the new use of old drugs for many years, and niclosamide and quinacrine are the drugs that we screened and have paid more attention to in anti-cancer field. In this study, we, for the first time, developed a new strategy for melanoma treatment using niclosamide and quinacrine to obtain the dramatic synergistic anticancer and investigated the underlying mechanism involved. Based on our novel findings, we concluded that niclosamide in combination of quinacrine exerted great anticancer effect with low concentration of each drugs against melanoma and other tumors through activating autophagy-mediated p53-dependent apoptosis. Meanwhile, the new strategy presents safety for the main normal tissue and organs in mice, and very low cytotoxicity for normal tissues derived primary cells or immortalized normal cell lines.

Methods

Cell lines and culture

Mouse melanoma B16 and B16-F10 cell lines, mouse breast cancer cell line 4T1, mouse kidney carcinoma cell line RENCA, human melanoma cell line A375, human prostate carcinoma cell line DU145, human kidney carcinoma cell line A498 and human bone marrow mesenchymal stem cells BMSCs were obtained from American Type Culture Collection (ATCC). Human oral gingival epithelial immortalized cell line SG were gifted by Professor Meng, Peking University School and Hospital of Stomatology. These cell lines were identified by STR profiling and maintained in Dulbecco's modified Eagle's medium (DMEM, Gibco, Carlsbad, CA, United States), with 10% fetal bovine serum (FBS; Gibco) and 1% streptomycin/penicillin (hereafter called complete medium). Cells were incubated in a 37 °C, 100% moist incubator containing 5% CO_2 atmosphere.

Optimal dose finding assay through IncuCyte ZOOM^{TM} monitor system

Cells were seeded in a 96-well plate at a density of 5×10^3 cells per well in 200 μL complete medium. At the following day, the cells were treated with different concentrations of niclosamide (Sigma-Aldrich, USA) dissolved in dimethylsulfoxide (DMSO, Sigma-Aldrich, United States) and/or quinacrine (Sigma-Aldrich, USA) dissolved in Milli-Q water and recorded every 4 h by IncuCyte ZOOM^{TM} (Essen BioScience, USA) for 48 h. The wells with vehicle DMSO treated cells served as control. The cell growth curve was calculated by continuous changes by cell confluence. The independent experiments were repeated three times and the cell growth rate was calculated based on the mean of cell confluence.

CCK8 assay

The cell proliferation was also measured using Cell Counting Kit-8 (CCK-8) assay. A total of 5000 cells in 100 μL complete medium were cultured in a 96-well plate, and there are three replications for each sample. Following overnight incubation, cells were cultured in complete medium containing indicated doses of niclosamide and/or quinacrine. 10 μL CCK-8 was mixed with 90 μL medium per well and incubated at 37 °C, 5% CO_2 for 30 min. Then the cell proliferation rate was determined by OD_{450} value at 0, 24, 48 h. The experiment was repeated three times.

Wound healing assay

Cells were seeded in a 6-well plate at a density of 2.5×10^5 cells per well in 2 mL complete medium. Once the cells reached 90% confluence, the cells were starved by 2 mL serum-free DMED for 24 h, scratched by 200 μL pipette tips. The detached cells were removed by rinsing twice with PBS. The remaining cells were treated with indicated doses of niclosamide and/or quinacrine for 24 h. Images were taken with an inverted fluorescence microscope at 10 × magnification to calculate the migration speed of the cells. The experiment was repeated three times.

Transwell invasion assay

The invasion ability of cancer cells was measured by Transwell assay with a Transwell chamber plate (8 μm pore size, Bedford, USA) and a polycarbonate membrane coated with 100 μL of diluted Matrigel (1:80 dilution, BD Biosciences, USA). Briefly, cells were starved for 24 h and about 1×10^5 cells in 100 μL serum-free DMED were seeded in the upper chamber, while the bottom chamber was filled with 500 μL DMEM contained 20% FBS. Indicated doses of niclosamide and/or quinacrine were added to the upper chamber. At 12 h after treatment, the cells were fixed by 95% ethanol, and dyed with 0.1% crystal violet, removed the

cells in the upper chamber by cotton swobs. Then migrated cells were photographed and counted by a light microscopy at 20 × magnification. The experiment was repeated three times.

Western blot assay

Proteins were extracted from cells which were treated with indicated drugs for 24 h by RIPA (Applygen Technologies, China) containing a phosphatase and protease inhibitors (Roche Diagnostics, USA). Briefly, 50 μg of total protein per well was loaded into a 12.5% SDS-PAGE (Biotides, China) for electrophoresis and then transferred to a 0.45 μm PVDF membranes (BioRad, USA). Next, the membranes were blocked by 5% skimmed milk for 1 h at 25 °C, and subsequently incubated with corresponding primary antibodies overnight at 4 °C. At the next day, after the membranes were incubated with corresponding HRP-conjugated secondary-antibodies for 1 h and then ECL solution for 1 min, the membranes were exposed by an ECL detection system (Applygen Technologies, China). The protein expression levels were determined by using the following primary antibodies against: cleaved-PARP (1:1000 dilution, Abclonal, China), cleaved-caspase3 (1:1000 dilution, Cell Signal Technology, USA), RPS18 (1:1000 dilution, Abclonal, China), LC3B (1:1000 dilution, Abclonal, China), p62 (1:1000 dilution, Beyotime, China) and p53 (1:1000 dilution, Proteintech, USA). Relative protein quantification normalized to RPS18 was carried out using the ImageJ software. The amount of each protein in controls was set to one.

Flow cytometric analysis of apoptosis

The cells were resuspended in 100 μL in Annexin V Binding Buffer (Biolegend, USA) at a concentration of 1.0×10^6 cells/mL. Thereafter, 5 μL of APC-Annexin V and 5 μL of 7-AAD Viability Staining Solution (Biolegend, USA) were added to each sample, respectively, and incubated for 15 min at room temperature in the dark. Then, 400 μL of Annexin V Binding Buffer were added to each tube. All samples were analyzed by flow cytometry with proper machine settings. The experiment was repeated three times.

Autophagy detection by Ad-mCherry-GFP-LC3B infection

Cells were grown on 6-well plates until they reached 20%–30% confluence and then infected with Ad-mCherry-GFP-LC3B adenovirus (Beyotime, Shanghai, China) at an MOI of 10 for 24 h at 37 °C. Based on the manufacture's instruction, the fusion protein of red fluorescent protein mCherry and LC3 can be effectively expressed in target cells after infection, which can be used for autophagy test. Under non-autophagy condition, mCherry-GFP-LC3B exists in the cytoplasm in the form of diffuse yellow fluorescence (the combined effect of mCherry and GFP). Once onset of autophagy, mCherry-GFP-LC3B aggregates on the autophagosome membrane and presents yellow dots. When the autophagosomes fuse with the lysosomes, mCherry-GFP-LC3B presents red spots due to partial quenching of GFP fluorescence in the acidic environment within the lysosomes. At 24 h after niclosamide plus quinacrine treatment, the images were taken with a fluorescence microscope and merged for determining autophagic status of the cells.

p53 knockdown using small interfering RNA

p53 siRNA and non-targeting siRNA were purchased from Guangzhou RiboBio Co, Ltd. (Guangzhou, China). For siRNA transfection, cells were seeded in 6-well plates, when they reached 70%-80% confluence, siRNAs were added into the cells with Lipo8000 reagent (Beyotime, Shanghai, China) according to the manufacturer's recommendations. The cells were then exposed to different drugs and harvested for the further experiments including western blot, and biological behavior studies.

Synergism analysis

Synergistic effect was evaluated based on the niclosamide and quinacrine combination index (CI) generated from CompuSyn software v1.0 (ComboSyn Incorporated, Paramus, NJ, USA). The CI value is used to determine whether niclosamide and quinacrine have the synergistic effect on tumor growth inhibition. CI <0.9 indicates synergism, CI between 0.9 and 1.1 means additive effect, and CI>1.1 antagonism.

Animal study

C57BL/6 mice (4-6 weeks old, weighting 20-25 g) were purchased from Beijing Vital River Laboratory Animal Technology (Beijing, China). The mice are kept in an environment of 22 ± 1 °C and a light/dark cycle of 12 h/12 h. All animal studies were done in compliance with the regulations and the Peking University institutional animal care guidelines and conducted according to the AAALAC and the IACUC guidelines (NO. LA2019011). All 24 mice were randomly divided into four groups: control group, niclosamide treatment group, quinacrine treatment group and combination group. B16 cells (2×10^5) were subcutaneously injected into the animal back. Body weight and tumor volume were measured every day in the 2 weeks' experiment period. When the allograft tumor reached 75–100 mm^3, niclosamide (200 mg/kg) were daily given by gavage administration in niclosamide group and combination group; quinacrine (50 mg/kg) was intraperitoneally injected into mice of quinacrine group and combination group every day. Meanwhile, mice in the control group were given daily intragastric gavage administration of equal volume of vehicle and intraperitoneal injection of physiological saline. At 2 weeks after treatment, the mice were euthanized, and the tumors were removed, weighed and recorded with a digital camera, then fixed immediately by 10% formalin.

In addition, the main organs including brain, kidney, spleen, liver, intestine were removed and fixed by 10% formalin for further biosafety evaluation through histopathological examination.

HE staining for histopathological examination

The fixed liver, brain, spleen, kidney, intestine and other tissues from the mice were dehydrated, embedded in paraffin, and sectioned to a thickness of 4 μm slide. The slides were deparaffinized with xylene and rehydrated with gradient alcohol. Then, slices were stained with hematoxylin for 5 min and eosin for 1 min, dehydrated with gradient alcohol, and finally mounted by neutral resin. All sections were observed and recorded by a microscope.

Immunohistochemistry

The fixed tumors were dehydrated, embedded in paraffin, and then sliced into 4 μm thick slices, deparaffinized with xylene and rehydrated with different concentrations of ethanol. Next, slices were heated in 0.01 mol/L sodium citrate buffer at 100 °C for 10 min to perform antigen retrieval. After inactivation of endogenous peroxidase by 3% H_2O_2, the slices were blocked with 10% goat serum and incubated with 50 μL diluted primary antibodies overnight at 4 °C. The Next day, slices were stained with HRP-labeled secondary antibody (ZSGB-BIO, Beijing, China) at 37 °C for 30 min. Finally, the sections were incubated with DAB for 3 min for color development. After counterstained with hematoxylin, all sections were observed and recorded by a microscope. A staining score was calculated by the staining intensity score (negative, weak, moderate, and strong scored as 0, 1, 2, and 3, respectively) multiplying the score of positively stained cell numbers (0, none; 1, 1–40%; 2, 40–70%; 3, 70–100%) [30].

Evaluation anti-cancer effect of niclosamide in combination with quinacrine in other cancer cell lines

Cancer cell lines including 4T1, RENCA, A375, DU145 and A498 were cultured in DMEM complete medium. A total of 5000 cells from each above cell line in 100 μL complete medium were inoculated in 96-well plates, and there are triplicates for each sample. Following overnight incubation, cells were cultured in complete medium containing indicated doses of niclosamide and/or quinacrine. IncuCyte ZOOM™ assay were performed to determine the anti-cancer effect of niclosamide in combination with quinacrine. The experiment was repeated three times.

Cytotoxicity evaluation by using normal primary cells and immortalized cell line

5000 cells of human oral gingival epithelial immortalized cell line SG and human bone marrow mesenchymal stem cell BMSCs were plated in triplicates in a 96-well plate with 100 μL complete medium per well, respectively. Following overnight incubation, cells were cultured in complete medium containing indicated doses of niclosamide and/or quinacrine. CCK8 assay were carried out to determine the cytotoxicity for normal cells. Apoptosis was detected by flow cytometry describe above. The experiment was repeated three times.

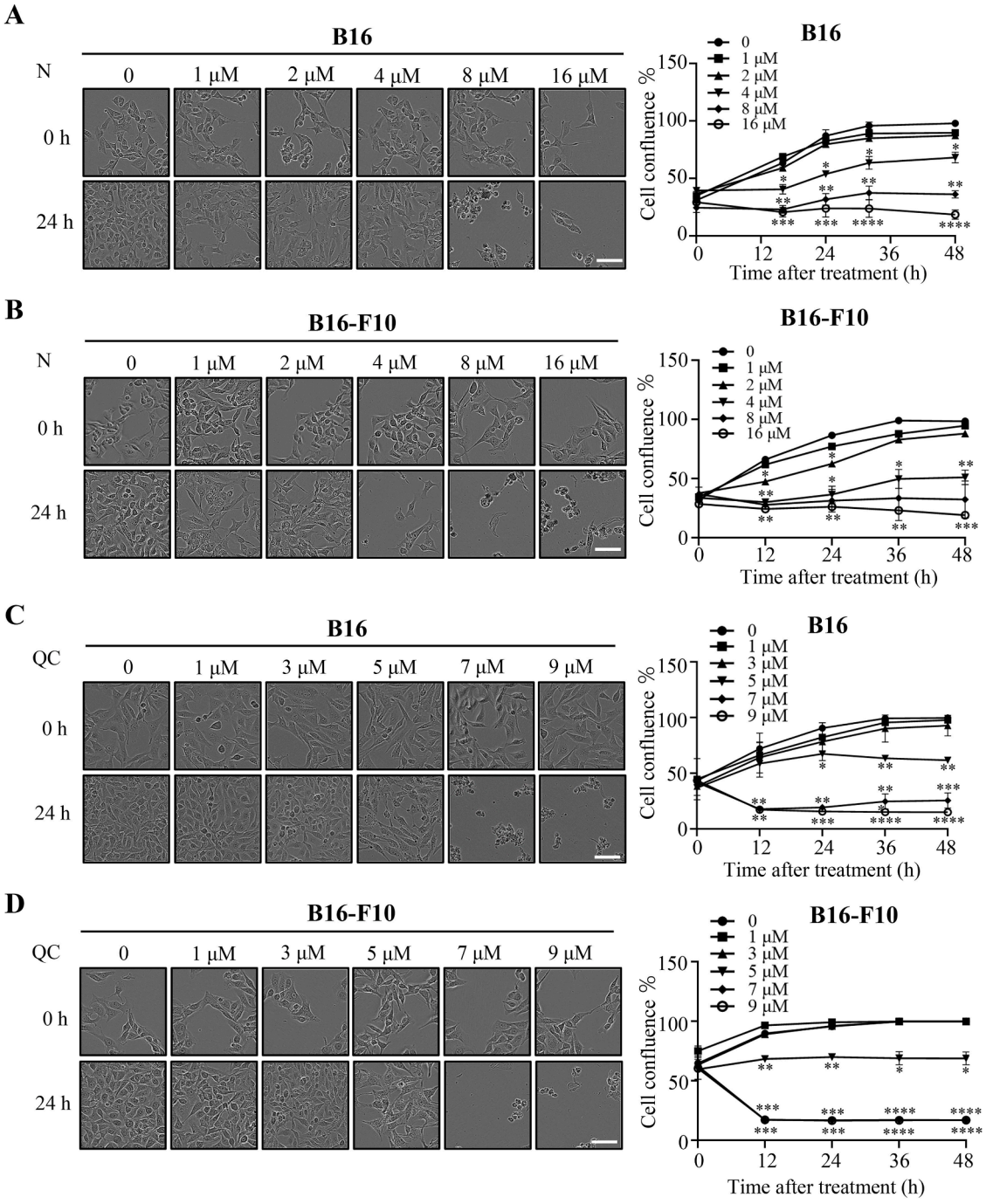

Fig. 1. Niclosamide (N) and quinacrine (QC) inhibit cell proliferation of B16 and B16-F10 cell lines at a dose-dependent manner. Images of B16 and B16-F10 treated with different doses of niclosamide and its growth curve **(A, B)**. Images of B16 and B16-F10 treated with different doses of quinacrine and its growth curve. **(C, D)**. (Scale bar: 100 μm) $^{*}P < 0.05$, $^{**}P < 0.01$, $^{***}P < 0.001$, $^{****}P < 0.0001$.

Statistical analysis

Data were presented means ± standard deviation (SD) obtained from three independent experiments. Statistical analysis was performed using GraphPad Prism v8.4 software. A nonparametric *t* test was used to compare continuous variables between two groups and the differences between groups were examined using an analysis of one-way analysis of variance (ANOVA). $P < 0.05$ was considered statistically significant.

Results

Niclosamide and quinacrine, respectively inhibit cell proliferation of B16 and B16-F10 cell lines at a dose-dependent manner

To detect whether niclosamide (N) and quinacrine (QC) have an effect on the growth of B16 and B16-F10 cell lines of melanoma, cell proliferation was determined by IncuCyte ZOOM™ Assay. The results showed that low-dose of N (≤2 μM) had no effect on B16 and B16-F10 cell lines, but it significantly attenuates cell growth at high concentrations (4, 8 and 16 μM) (Fig. 1A&B). Similar results were observed in QC-treated cells, which high doses of QC (7 and 9 μM) exert inhibiting effects on cell proliferation (Fig. 1C&D). These data suggested that N and QC exhibited dose-dependent inhibiting effects on melanoma cell lines.

Low doses of niclosamide and quinacrine combination significantly inhibits the proliferation, migration and invasion ability of melanoma cell lines

To investigate whether the two drugs have a synergistic effect, we used IncuCyte ZOOM™, CCK8, wound healing and Transwell invasion assays to determine cell proliferation, migration, and invasion capabilities. IncuCyte ZOOM™ assay showed that a low dose of N or QC did not influence the cell growth compared with the control group, however, the combined treatment of N (1.5 μM) and QC (3 μM) dramatically inhibit the cell proliferation of B16 and B16-F10 (Fig. 2A&B). Consistently, CCK8 assays showed that low-dose of N and QC combination significantly inhibited the cell growth rates of mouse melanoma cell lines B16, B16-F10 and human melanoma cell line A375 (Fig. 2C–E). Meanwhile, synergy analysis showed combination index (CI) of niclosamide and quinacrine at the default isobologram effect level Fa=0.5, 50% effective dose (ED50) condition, CI value was 0.09547, much lower than 1, which indicated that niclosamide and quinacrine have the strong synergistic effect on melanoma cell growth inhibition (Supplementary Fig. S1).

To further figure out the effects of the two drugs on melanoma cell lines, wound healing and Transwell invasion assays were used to determine the cell mobility after the treatment of N and QC. B16 and B16-F10 showed a significant decrease migration and invasion abilities after treated with 1.5 μM niclosamide and 3 μM quinacrine (Fig. 2 F–I). These data demonstrated that the combination usage of N and QC significantly suppressed the cell growth and mobility of melanoma cell lines.

Low doses of niclosamide and quinacrine combination induces apoptosis and autophagy of B16 and B16-F10

To explore the underlying mechanism regarding why the N combined with QC yields dramatic anti-cancer effects, we detected whether the combination drug induces cell death or cell cycle arrest in melanoma cells. Cell death-related proteins were chosen to identify the cell death, including p53, cleaved caspase-3 (c-CASP3) and cleaved PARP (c-PARP) (Other cell death-related protein expression presented in the Supplementary Fig. S2). B16 and B16-F10 cell lines were divided into 4 groups and treated with 0, 1.5 μM niclosamide, 5 μM quinacrine and their combination for 24 h. Flow cytometry assay demonstrated that the percentage of apoptotic cells of the drug-combined group is higher than the other groups in melanoma cell lines (Fig. 3A). Moreover, western blot results showed that protein p53, c-caspase3 and c-PARP were significantly up-regulated in the combined group, compared with the control and drug-alone groups (Fig. 3B).

Since other antimalarial drugs have previously been shown to modulate autophagy, we tested whether the combination of niclosamide and quinacrine in low concentrations was able to induce autophagy in addition to promoting apoptosis. As is shown in Fig. 3C, the expression of autophagic marker proteins LC3B was significantly up-regulated, and p62 was markedly down-regulated. This induction of LC3B and degradation of p62 are considered hallmarks of autophagic activation. To further evaluate the low doses of niclosamide and quinacrine combination-induced autophagy, we also used autophagy indicator tool Ad-mCherry-GFP-LC3B (Beyotime, China) to detect autophagic flux. Under the condition of setting the fixed fluorescence photography parameters, the results clearly showed an increased expression of yellow (autophagosome stage) and red (the stage of autophagosome fusion with the lysosome) dots fluorescence intensity in the combination group (Fig. 3D).

However, it was still unknown whether these results represented an increased production of autophagosome or inhibition of autophagosome and lysosome fusion. To verify whether niclosamide and quinacrine treatment increased autophagic flux, B16 and B16-F110 cells were treated with niclosamide and quinacrine in the presence or absence of bafilomycin A1(Baf-A1) (Selleck Chemicals, Shanghai, China), a potent autophagy inhibitor. Western blot assays showed that the expression levels of LC3B and p62 were rescued when the autophagy was repressed (Fig. 3E), confirming that niclosamide combined with quinacrine directly induced cell autophagy in melanoma cell lines.

Low doses of niclosamide and quinacrine combination-induced apoptosis depends on the activation of cell autophagy

Through the above experimental results, we knew that the niclosamide and quinacrine synergistically exerted their effect on melanoma cells by activating cell apoptosis and autophagy. Next, we sought to further explore the underlying crosstalk in the tumor cells infiltrated with low doses of niclosamide and quinacrine combination.

On the one hand, to explore whether autophagy could affect apoptosis in this situation, autophagy inhibitor Baf-A1 was used to block autophagy flux and then apoptotic markers were detected in the tumor cells with an inactive autophagy status. The western blot results showed that, after Baf-A1 treatment, the expression of apoptosis-related biomarkers p53, cleaved (c)-caspase 3 and c-PARP was dramatically down-regulated (Fig. 4A). Flow cytometry results showed that the percentage of apoptotic cells was significantly decreased too (Fig. 4B). This suggested that the occurrence of apoptosis may depend on the activation of niclosamide and quinacrine combination-induced autophagy.

On the other hand, knockdown of p53 by siRNAs specifically targeted to p53 was performed to assess whether apoptosis could affect autophagy in turn. Western blot results clearly showed that the three siRNAs for p53 could markedly knocked down p53 expression. Hereafter, siP53-1 was chosen for the following assays (Fig. 5A). The flow cytometry and western blot both showed that the p53-dependent apoptosis was partly suppressed in the p53 knockdown cells (Fig. 5B&C). However, LC3B and p62 proteins had little changes at the protein expression level (Fig. 5C). Consistently, after knockdown of p53 by siP53, the results of autophagy detection by Ad-mCherry-GFP-LC3B infection showed that the expression of red and green fusion protein did not change markedly in B16 cells ($P > 0.05$, compared with siNC) (Fig. 5D). Taken together, we found that apoptosis did not mediate the occurrence of autophagy in the combination group.

Low doses of niclosamide and quinacrine combination exerts similar effect on breast, prostate and kidney cancer cell lines, but shows a relatively low cytotoxicity on normal cells

To verify whether the synergistic effect of the low doses of

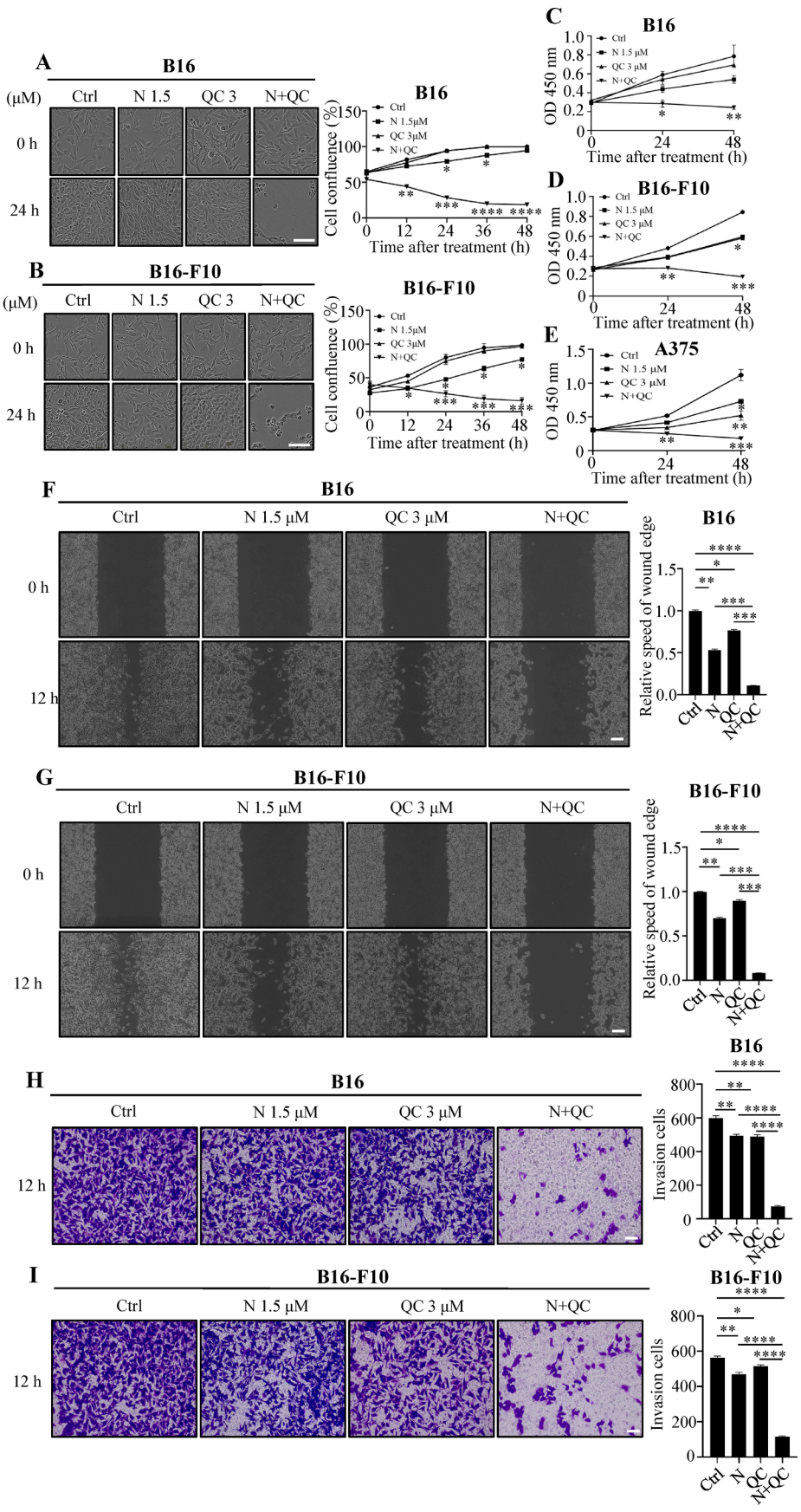

Fig. 2. Cell growth, migration and invasion in B16 and B16-F10 with different drugs treated. Images of B16 and B16-F10 treated with niclosamide (N, 1.5 μM) and/or quinacrine (QC, 3 μM) and their growth curve **(A, B)** (Scale bar: 100 μm). Growth rate of 1.5 μM N and/or 3 μM QC treated B16 B16-F10 and A375. **(C–E)**. Images of migration and invasion of 1.5 μM N and/or 3 μM QC treated B16 and B16-F10 cells **(F–I)**. (Scale bar: 200 μm). *, $P < 0.05$; **, $P < 0.01$; ***, $P < 0.001$; ****, $P < 0.0001$.

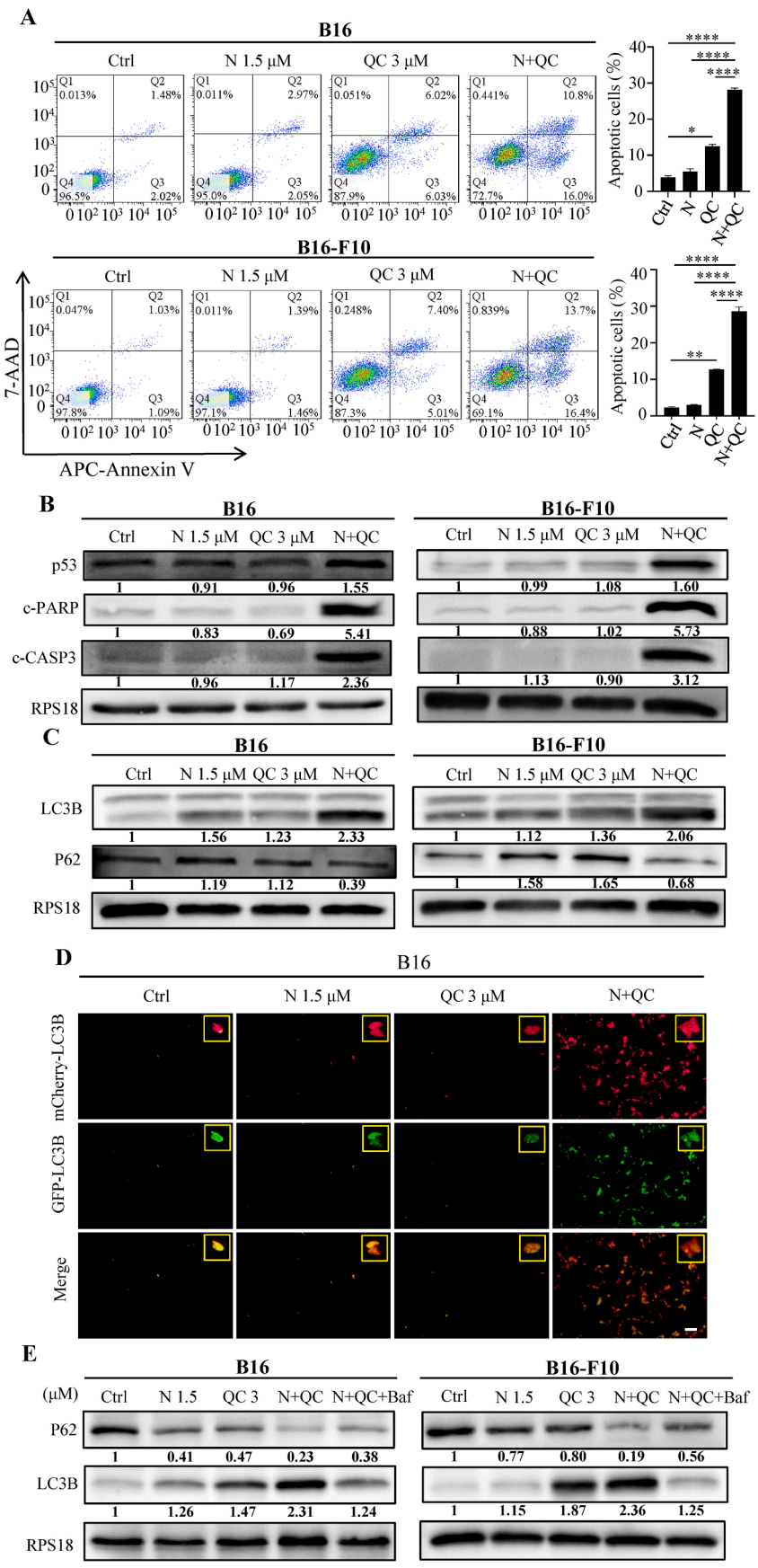

Fig. 3. Combination of niclosamide (N) and quinacrine (QC) induces cell apoptosis and autophagy. Representative images of APC-Annexin V/7-AAD flow cytometry in drug treated B16 and B16-F10 cell lines. The areas of Q2 and Q3 are considered as apoptotic cells **(A)**. Expression of apoptosis-related genes p53, c-PARP, c-CASP3 at protein level. The numbers below the bands represent relative quantification of each protein **(B)**. Expression of cell autophagy-related proteins LC3B and p62. The numbers below the bands represent relative quantification of each protein **(C)**. Representative images of fusion protein of red fluorescent protein mCherry and LC3, which indicated the autophagy flux after drug treatment. Pictures were taken under the condition of setting the fixed fluorescence photography parameters **(D)** (scale bar: 100 μm). The expression of LC3B and p62 in protein level upon a potent autophagy inhibitor Baf-A1 treatment. The numbers below the bands represent relative protein quantification **(E)**. *, $P < 0.05$; **, $P < 0.01$; ***, $P < 0.001$; ****, $P < 0.0001$.

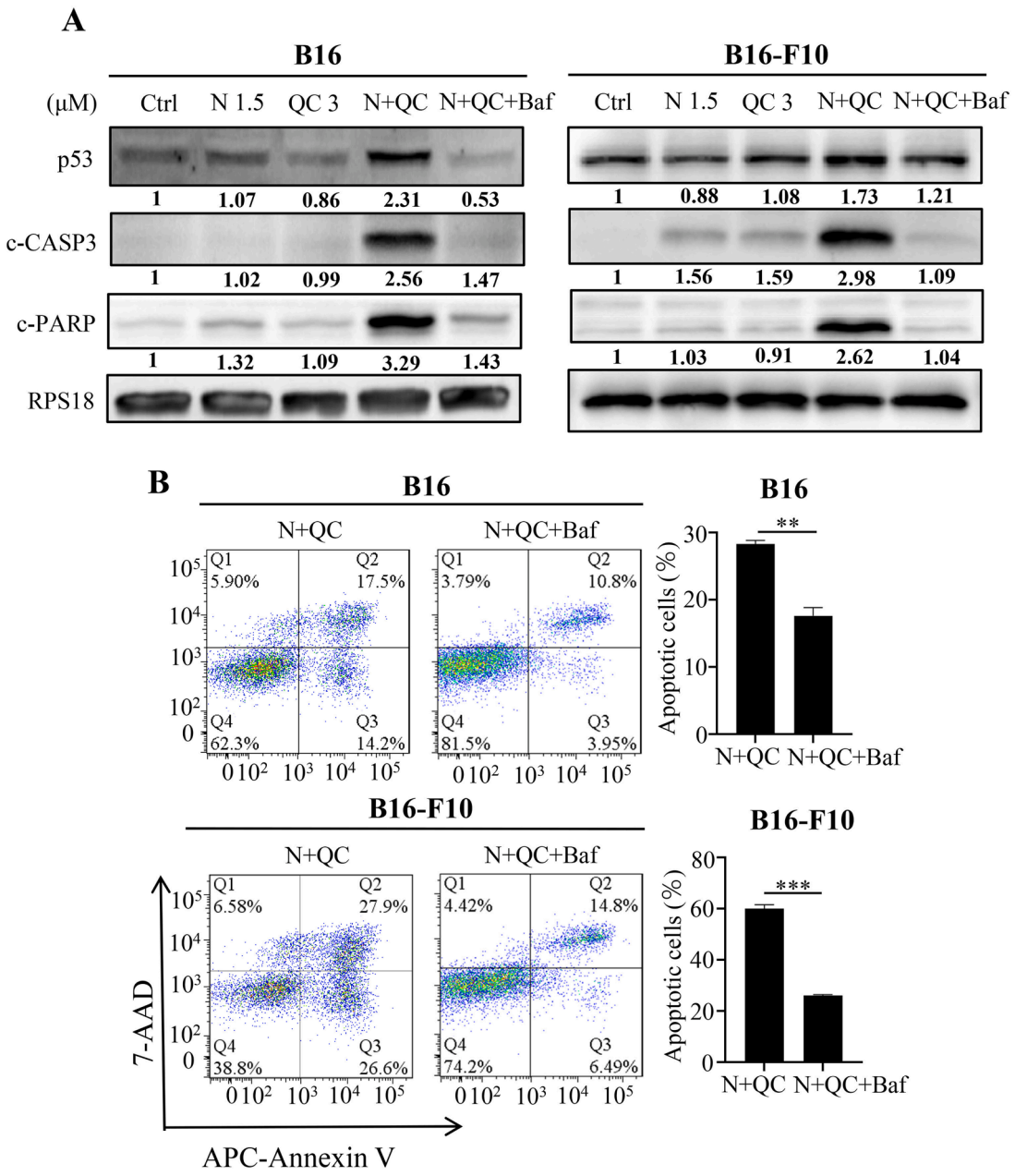

Fig. 4. Combination of niclosamide (N) and quinacrine (QC) induces apoptosis is partially suppressed by Baf-A1. The expression of apoptosis-related genes p53, c-PARP, c-CASP3 at protein level under a potent autophagy inhibitor Baf-A1 treatment. The numbers below the bands represent relative protein quantification**(A)**. Apoptosis results showed that representative images of APC-Annexin V/7-AAD flow cytometry in N and QC treated B16 and B16-F10 with or without Baf-A1 treatment **(B)**. *, $P < 0.05$; **, $P < 0.01$; ***, $P < 0.001$; ****, $P < 0.0001$.

niclosamide and quinacrine combination was also effective on other tumor cells as a universal strategy role of the anti-cancer drug. We choose the mouse breast cancer cell line 4T1, human prostate cancer cell line DU145, human kidney cancer cell line A498, and mouse kidney cancer cell line Renca. IncuCyte ZOOM^{TM} assay showed that niclosamide at a concentration of 1.5 μM and quinacrine at a concentration of 3 μM could synergistically inhibited the proliferation ability of these cell lines and caused the cell death like melanoma cell lines B16 and B16-F10 described above (Fig. 6A–D). To sum up, the synergistic effect of niclosamide and quinacrine may be as a novel universal anti-cancer strategy for cancer treatment.

Meanwhile, in order to verify whether the synergistic effect of the low doses of niclosamide and quinacrine combination was effective on normal cells, we choose human gingival epithelial cell line (SG) and bone marrow mesenchymal stem cells (BMSCs). CCK8 assay showed that the toxic effect of the combination drug on normal cells was relatively slight compared with B16-F10. The combination reduced about 23% of SG proliferation, 26% of BMSCs cell growth rate at 48 h after treatment (Fig. 6E). Consistently, the number of apoptotic cells induced by the combination therapy was only increased slightly (less than 2.79%) in immortalized epithelial cell line SG, and not changed in BMSCs at 24 h after treatment (Fig. 6F).

Low doses of niclosamide and quinacrine combination exerts anti-melanoma role in vivo

To verify the effects of combined usage *in vivo*, C57BL/6 mice were subcutaneously injected with B16 cells. The tumors were smaller in size and lighter in weight in the combined group, compared with the other three groups (Fig. 7A–C). Furthermore, the immunohistochemistry

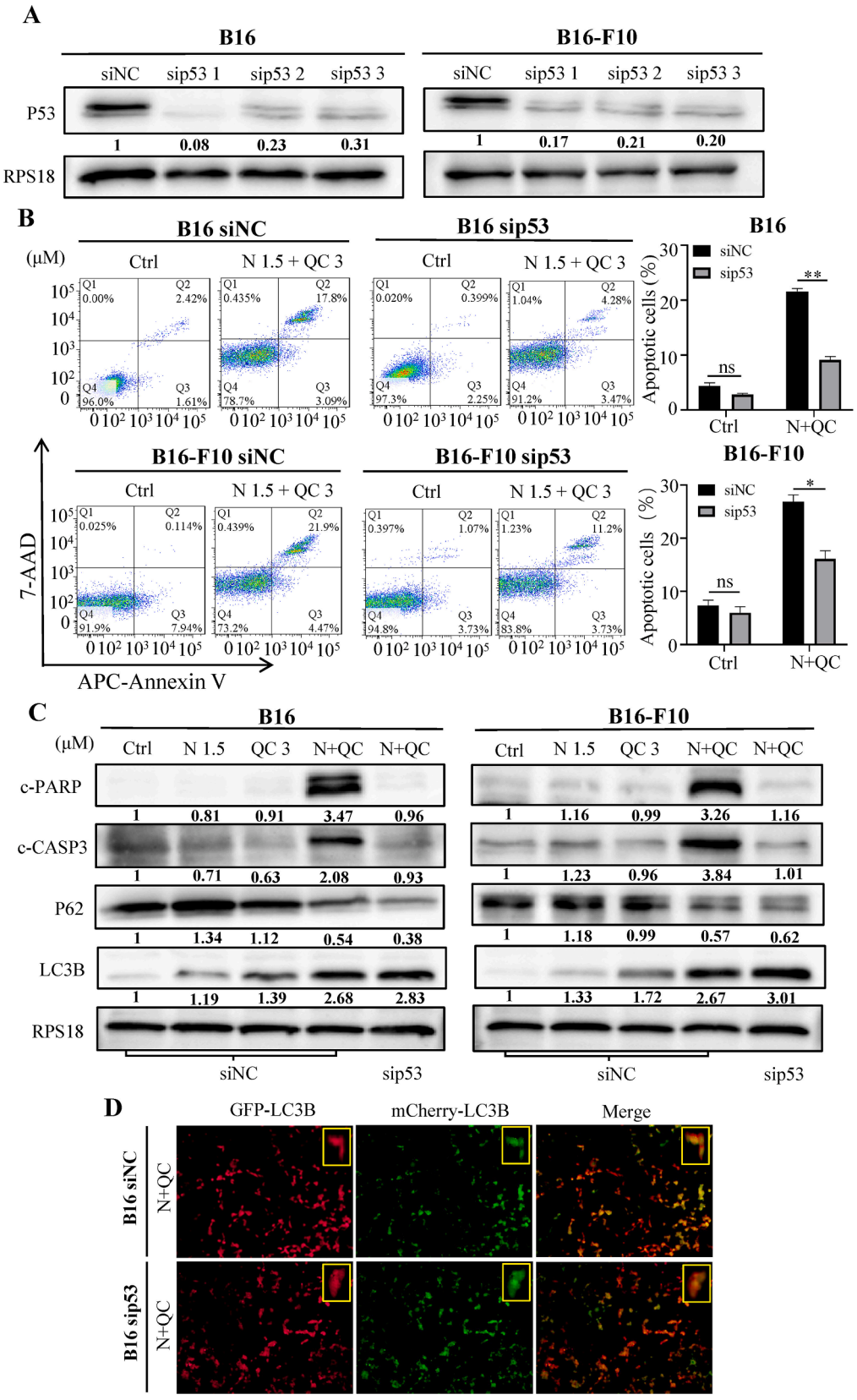

Fig. 5. p53 knockdown partially inhibits cell apoptosis but does not influence cell autophagy. Efficiency of p53 knockdown of B16 and B16-F10 at protein level. The numbers below the bands represent relative protein quantification**(A)**. Representative flow cytometry images of APC-Annexin V/7-AAD in N and QC-treated B16 and B16-F10 cells after knockdown of p53 by siRNA **(B)**. The expression of apoptotic-related proteins c-CASP3 and c-PARP, and autophagy-related proteins LC3B and p62 in B16 and B16-F10 cells after knockdown of p53 by siRNA. The numbers below the bands represent relative protein quantification **(C)**. After knockdown of p53 by siP53, the results of autophagy shows that the fusion protein of red fluorescent protein mCherry and LC3, and GFP expression pattern did not change markedly, compared with siNC ($P > 0.05$). The enlarged images were shown at the right concern of each picture **(D)**. *, $P < 0.05$; **, $P < 0.01$.

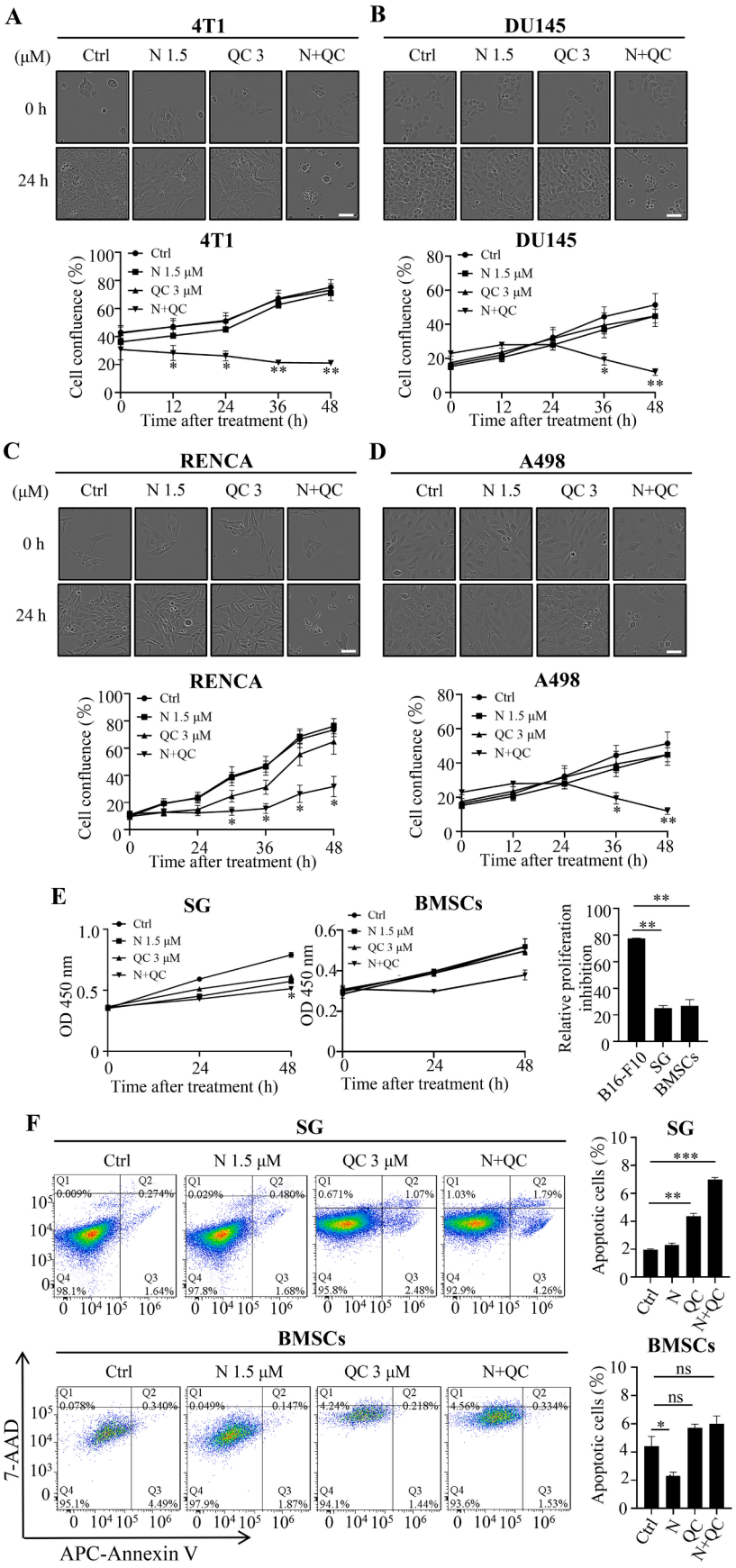

Fig. 6. Synergistic effect of niclosamide (N) and quinacrine (QC) combination also works on other cancer cell lines, but shows a low toxicity on normal cells. Images of tumor cell lines (4T1, DU145, RENCA and A498) and immortalized epithelial cell line SG and normal primary cells BMSCs treated with N and QC and their growth curve. **(A-E)** (Scale bar: 100 μm). Apoptosis detection by flow cytometry shows that the representative images of APC-Annexin V/7-AAD in N plus QC treated SG and BMSCs **(F)**. *, $P < 0.05$; **, $P < 0.01$.

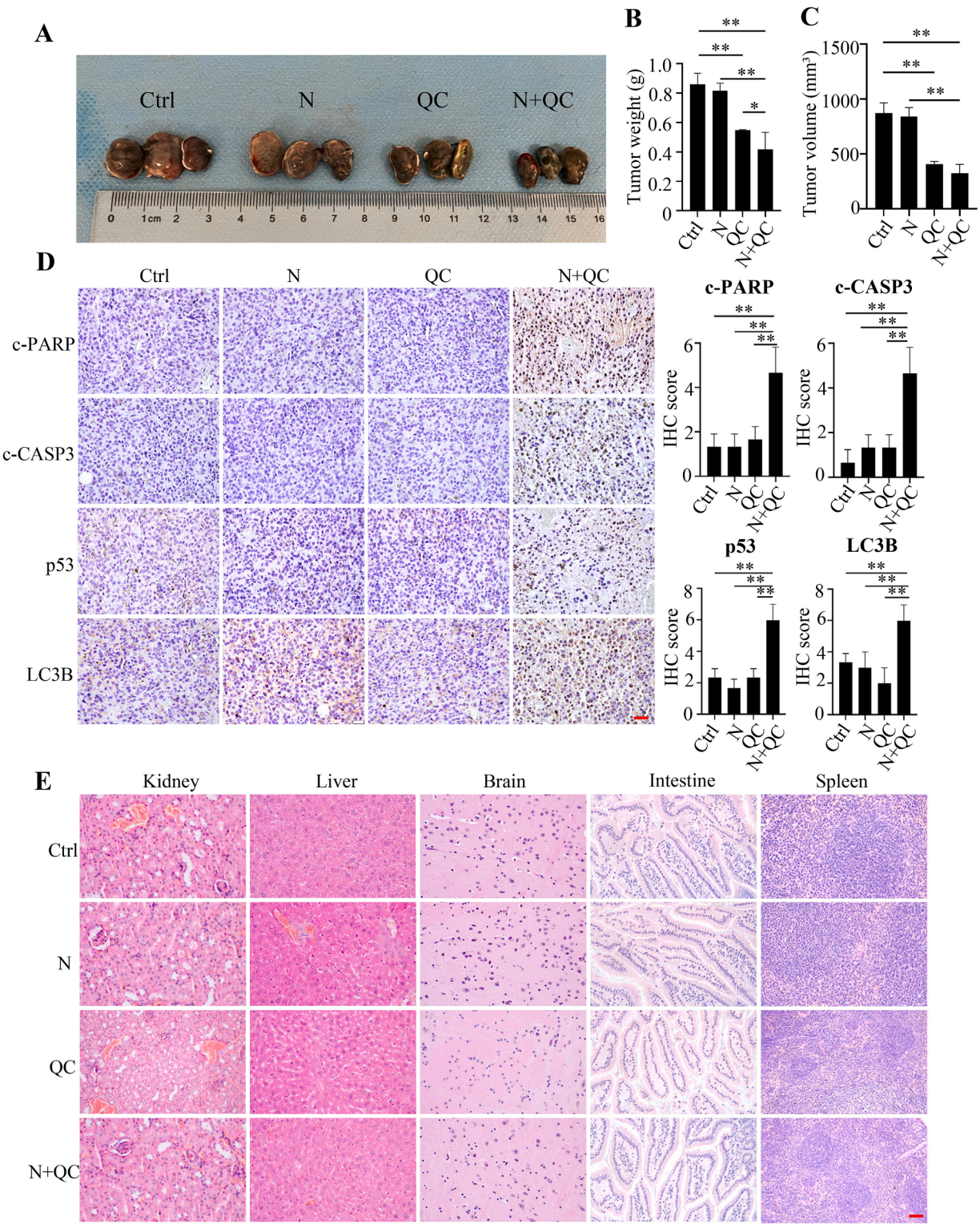

Fig. 7. Co-treatment of niclosamide (N) and quinacrine (QC) shows a synergistic effect *in vivo*. Representative images of B16-derived allografts of different drugs treated groups **(A)**. Weight and volume of tumors in different groups **(B, C)**. Immunohistochemistry and statistical analysis of c-PARP, c-CASP3, p53 and LC3B. **(D)**. HE staining photos of the tissues obtained from different groups **(E)**. (Scale bar: 200 μm) *, $P < 0.05$; **, $P < 0.01$.

results showed that niclosamide and quinacrine combination treatment markedly increased the c-PARP, c-CASP3, p53 and LC3B positive stained tumor cells compared to other groups (Fig. 7D), which indicated that niclosamide and quinacrine combination induced apoptosis and autophagy of tumor cells and was in line with the *in vitro* results (Fig. 3B&C). Importantly, aberrant pathology was merely observed in normal tissues including kidney, live, brain, intestine and spleen (Fig. 7E), indicating a minimal toxicity of the two drugs at a low dose combination within normal tissues.

Discussion

Malignant melanoma is one of the most lethal types of cancer with a dramatic increase of its incidence in the last 50 years. There are about 6700 new melanoma cases in our country per year, and the death toll is as high as 3200 cases [31]. Melanoma in early stage can be treated by surgical removal, but advanced stages of melanoma has already metastasized to other organs such as lung and bone and cannot be completely removed. In the past 5 years, however, treatment options for patients with metastatic melanoma, especially BRAF-mutant melanoma, have dramatically changed with the emerging of eight new therapeutic agents which gained FDA approval. The RAS–RAF–MEK–ERK signaling cascade is one of the most mutated pathways in human cancers and approximately 50% of melanoma patients possess a druggable hotspot V600E/K mutation in the BRAF protein kinase [32–34], targeted therapy directed against BRAF and MEK mutations have been one of the primary therapies of malignant melanoma patients over the past decade and improved their prognosis to some extent [35]. Besides, immunotherapies,such as CTLA-4 and PD-1 monoclonal antibodies which work for metastatic melanoma by stimulating or regulating the body's immune system as well as improving microenvironment, also achieved promising outcomes in malignant melanoma [36]. However, A number of studies have confirmed that targeted drugs are prone to cause some serious side effects: skin toxicity injuries, joint pain, hair loss and diarrhea during the process of treatment, and excessive use of targeted drugs may also cause skin squamous cell carcinoma, skin basal cell carcinoma and other tumors. Similarly, the adverse immune side effects of immunotherapy are often fatal for patients with advanced tumors [37,38]. Therefore, it is of great significance to find out new treatment strategy with small side effects and remarkable consequences. Conventional drug in new use is greatly promising due to its biological safety and proper economic cost [5].

The anti-tapeworm drug niclosamide and the anti-malarial drug quinacrine are two Food and Drug Administration (FDA)-approved drugs, which both exhibit optimistic safety profile and low toxicity even after long-term exposure in animals. Numerous studies have showed that both niclosamide [39] and quinacrine [22] alone or combined with cisplatin could dramatically inhibit cancer cell growth ability and induce cell death even at a low concentration, implying that niclosamide and quinacrine have the potential to be good anti-cancer agents. To date, no study tests the combination of niclosamide and quinacrine in cancer treatment.

In this study, we, for the first time, reported the anti-cancer properties of the niclosamide and quinacrine in melanoma, evaluated their synergistic effect and explored the underlying molecular mechanism involved.

The first new finding of the study is that low doses of niclosamide and quinacrine combination can cause dramatically anti-cancer effects on melanoma, but low cytotoxicity to normal cells and mice, which indicates that the two drugs have good biological safety.

In our research, we found that the combination of drugs can inhibit the proliferation, migration and invasion of melanoma tumor cells, and cause cell death. However, the toxic effect on normal cells was far less than tumor cells. In animal experiments, we found that there was no significant difference in the mental state of the mice in each group. HE staining also proved that the combined medication did not cause significant toxic side effects on the organs of the mice.

The second new finding of the study is that we found the novel mechanism regarding low doses of niclosamide and quinacrine combination yields synergistic effect in melanoma via activating autophagy-mediated p53-dependent apoptosis.

Co-treatment of niclosamide and quinacrine effectively caused apoptosis and promoted autophagy across two mouse melanoma cell lines B16 and B16-F10 *in vitro* as well as *in vivo* in mouse-derived allografts. In cancer, autophagy can play dual a role in different types and stages of cancer, including tumor suppressive and tumor-promoting which is determined by nutrition supply, stress of tumor microenvironment, pathogenic conditions, and the state of immune system [21]. Our findings show that an exposure to niclosamide and quinacrine leads to autophagosome formation, LC3B accumulation and p62 down-regulation, all of which are hallmarks of autophagy. We also found that combination of niclosamide and quinacrine can up-regulated c-CASP3, c-PARP and p53. Furthermore, flow cytometry showed an increase in the proportion of apoptotic cells of the combination group, all of which suggested cell apoptosis.

To detect whether co-treatment of niclosamide and quinacrine induced-autophagy and apoptosis are independent or related to each other, first of all, we chemically blocked autophagy using an autophagy inhibitor bafilomycin A (Baf-A1), niclosamide and quinacrine-mediated apoptosis is subsequently attenuated both in cellular and molecular levels. P53, a tumor suppressor protein, controls the cell cycle, DNA replication, as well as abnormal cell division during tumor growth [40]. Usually, p53 are turned off and expressed when the cells sustain stress, uncontrolled division and proliferation, When the damage is beyond tissue repair capability, p53 activates apoptosis by triggering apoptosis-involved genes [41]. Our finding shows an increase expression of p53 protein in the combination group. In order to detect the role of p53 in the synergy effect, genetic silence of p53 expression by siRNA in the melanoma cell lines. We observe less apoptosis-related protein expression and less apoptotic cells, but autophagy-related protein expression as well as cell autophagy did not change obviously, which suggests the combination drugs play a synergistic effect in melanoma by activating autophagy-mediated p53-dependent apoptosis. Considering that the effect is very clear, autophagy-mediated p53-dependent apoptosis may be an innovation in the field of cancer treatment targets.

The third new finding of the study is that we probably verify the universal anti-cancer role of low doses of niclosamide and quinacrine combination in other cancer cell lines. The new findings broaden our understanding of the anti-cancer effect of niclosamide and quinacrine. Importantly, through *in vitro* (the immortalized epithelial cell line and BMSCs) and *in vivo* (animal study) assay, we found the new strategy only show a slight cytotoxicity to epithelial cells and did not show any toxicity in mice. Low doses of each anti-cancer drugs mean less cytotoxicity to normal cells, tissues and organs in human, which may reduce cancer patient concerns about chemotherapy toxicity. In addition, considering that niclosamide and quinacrine are the two low-cost drugs, which may help reduce the treatment cost of cancer patients. Collectively, our data indicate that we may develop a novel safe chemotherapeutic strategy for all types of cancer treatment.

Conclusion

In summary, our data, for the first time, not only provide the direct evidence and new melanoma treatment strategy that co-treatment of niclosamide and quinacrine synergistically inhibited proliferation, migration and invasion ability of melanoma cell lines, but also highlight the underlying mechanism of niclosamide and quinacrine-mediated autophagy-activated p53-dependent apoptosis, which may be developed a novel, universal and safe chemotherapeutic strategy for cancer treatment.

Ethics statement

The animal study carried out in accordance with the Institutional Animal Care and Use Committee at Peking University Health Center. The protocol (LA2020012) was approved by the "Ethnic Committee of Peking University Health Center."

Consent for publication

Not applicable.

Availability of data and materials

All data analyzed are included in this paper as well as the supplementary file.

Funding

The study was supported by the Research Grants from the National Nature Science Foundation of China (Grant Nos. 81970920, 81900983 and 81772873), the National Key Research and Development plan of the Natural Science Foundation of Beijing Municipality (Grant No. 7182181), and the Shanghai Science and Technology Young Talents Sailing Program (19YF1442500).

CRediT authorship contribution statement

Xuan Zheng: Investigation, Data curation, Writing – original draft, Writing – review & editing. **Jianyun Zhang:** Investigation, Data curation, Writing – review & editing. **Shuangting Li:** Investigation, Data curation, Writing – review & editing. **Xiaolei Gao:** Investigation, Data curation, Writing – review & editing. **Yixin Zhang:** Investigation, Data curation, Writing – review & editing. **Meng Wang:** Investigation, Data curation, Writing – review & editing. **Liying Dong:** Investigation, Data curation, Writing – review & editing. **Liangjie Sun:** Investigation, Data curation, Writing – review & editing. **Na Zhao:** Investigation, Data curation, Writing – review & editing. **Zeyun Ma:** Visualization, Writing – review & editing. **Chong Ding:** Visualization, Writing – review & editing. **Yixiang Wang:** Visualization, Writing – review & editing.

Declaration of Competing Interest

None declared.

Acknowledgments

Not applicable.

Supplementary materials

Supplementary material associated with this article can be found, in the online version, at doi:10.1016/j.tranon.2022.101425.

References

[1] S.N. Markovic, L.A. Erickson, R.D. Rao, R.H. Weenig, B.A. Pockaj, A. Bardia, C. M. Vachon, S.E. Schild, R.R. McWilliams, J.L. Hand, S.D. Laman, L.A. Kottschade, W.J. Maples, M.R. Pittelkow, J.S. Pulido, J.D. Cameron, E.T. Creagan, C. Melanoma Study Group of the Mayo Clinic Cancer, Malignant melanoma in the 21st century, part 1: epidemiology, risk factors, screening, prevention, and diagnosis, Mayo Clin. Proc. 82 (2007) 364–380.

[2] D. Schadendorf, A.C.J. van Akkooi, C. Berking, K.G. Griewank, R. Gutzmer, A. Hauschild, A. Stang, A. Roesch, S. Ugurel, Melanoma, Lancet 392 (2018) 971–984.

[3] R.L. Siegel, K.D. Miller, A. Jemal, Cancer statistics, 2020, CA Cancer J. Clin. 70 (2020) 7–30.

[4] A. Caldaria, R. Giuffrida, N. di Meo, L. Massari, C. Dianzani, S.P. Cannavo, F. Degrassi, E. Casablanca, I. Zalaudek, C. Conforti, Diagnosis and treatment of melanoma bone metastasis: a multidisciplinary approach, Dermatol. Ther. 33 (2020) e14193.

[5] S. Pushpakom, F. Iorio, P.A. Eyers, K.J. Escott, S. Hopper, A. Wells, A. Doig, T. Guilliams, J. Latimer, C. McNamee, A. Norris, P. Sanseau, D. Cavalla, M. Pirmohamed, Drug repurposing: progress, challenges and recommendations, Nat. Rev. Drug Discov. 18 (2019) 41–58.

[6] E.J. Barbosa, R. Lobenberg, G.L.B. de Araujo, N.A. Bou-Chacra, Niclosamide repositioning for treating cancer: challenges and nano-based drug delivery opportunities, Eur. J. Pharm. Biopharm. 141 (2019) 58–69.

[7] W. Chen, R.A. Mook Jr., R.T. Premont, J. Wang, Niclosamide: beyond an antihelminthic drug, Cell Signal 41 (2018) 89–96.

[8] Y. Li, P.K. Li, M.J. Roberts, R.C. Arend, R.S. Samant, D.J. Buchsbaum, Multi-targeted therapy of cancer by niclosamide: a new application for an old drug, Cancer Lett. 349 (2014) 8–14.

[9] U. Sack, W. Walther, D. Scudiero, M. Selby, D. Kobelt, M. Lemm, I. Fichtner, P. M. Schlag, R.H. Shoemaker, U. Stein, Novel effect of antihelminthic niclosamide on S100A4-mediated metastatic progression in colon cancer, J. Natl. Cancer Inst. 103 (2011) 1018–1036.

[10] M. Li, B. Khambu, H. Zhang, J.H. Kang, X. Chen, D. Chen, L. Vollmer, P.Q. Liu, A. Vogt, X.M. Yin, Suppression of lysosome function induces autophagy via a feedback down-regulation of MTOR complex 1 (MTORC1) activity, J. Biol. Chem. 288 (2013) 35769–35780.

[11] X. Li, R. Ding, Z. Han, Z. Ma, Y. Wang, Targeting of cell cycle and let-7a/STAT3 pathway by niclosamide inhibits proliferation, migration and invasion in oral squamous cell carcinoma cells, Biomed. Pharmacother. 96 (2017) 434–442.

[12] Y. Jin, Z. Lu, K. Ding, J. Li, X. Du, C. Chen, X. Sun, Y. Wu, J. Zhou, J. Pan, Antineoplastic mechanisms of niclosamide in acute myelogenous leukemia stem cells: inactivation of the NF-kappaB pathway and generation of reactive oxygen species, Cancer Res. 70 (2010) 2516–2527.

[13] A. Wieland, D. Trageser, S. Gogolok, R. Reinartz, H. Hofer, M. Keller, A. Leinhaas, R. Schelle, S. Normann, L. Klaas, A. Waha, P. Koch, R. Fimmers, T. Pietsch, A. T. Yachnis, D.W. Pincus, D.A. Steindler, O. Brustle, M. Simon, M. Glas, B. Scheffler, Anticancer effects of niclosamide in human glioblastoma, Clin. Cancer Res. 19 (2013) 4124–4136.

[14] K. Gurova, New hopes from old drugs: revisiting DNA-binding small molecules as anticancer agents, Future Oncol. 5 (2009) 1685–1704.

[15] D.B. Oien, C.L. Pathoulas, U. Ray, P. Thirusangu, E. Kalogera, V. Shridhar, Repurposing quinacrine for treatment-refractory cancer, Semin. Cancer Biol. 68 (2021) 21–30.

[16] M.M. Billah, E.G. Lapetina, P. Cuatrecasas, Phospholipase A2 activity specific for phosphatidic acid. a possible mechanism for the production of arachidonic acid in platelets, J. Biol. Chem. 256 (1981) 5399–5403.

[17] V.D. Mouchlis, E.A. Dennis, Phospholipase A2 catalysis and lipid mediator lipidomics, Biochim. Biophys. Acta Mol. Cell Biol. Lipids 1864 (2019) 766–771.

[18] P. Kalinski, Regulation of immune responses by prostaglandin E2, J. Immunol. 188 (2012) 21–28.

[19] F. Mudassar, H. Shen, G. O'Neill, E. Hau, Targeting tumor hypoxia and mitochondrial metabolism with anti-parasitic drugs to improve radiation response in high-grade gliomas, J. Exp. Clin. Cancer Res. 39 (2020) 208.

[20] R. Liang, Y. Yao, G. Wang, E. Yue, G. Yang, X. Qi, Y. Wang, L. Zhao, T. Zheng, Y. Zhang, E. Wenge Wang, Repositioning quinacrine toward treatment of ovarian cancer by rational combination with TRAIL, Front. Oncol. 10 (1118) (2020).

[21] X. Li, S. He, B. Ma, Autophagy and autophagy-related proteins in cancer, Mol. Cancer 19 (2020) 12.

[22] A Khurana, D Roy, E Kalogera, Quinacrine promotes autophagic cell death and chemosensitivity in ovarian cancer and attenuates tumor growth, Oncotarget 2 (6) (2015) 36354–36369.

[23] D. Tang, R. Kang, T.V. Berghe, P. Vandenabeele, G. Kroemer, The molecular machinery of regulated cell death, Cell Res. 29 (2019) 347–364.

[24] E.A. Miao, J.V. Rajan, A. Aderem, Caspase-1-induced pyroptotic cell death, Immunol. Rev. 243 (2011) 206–214.

[25] L. Galluzzi, O. Kepp, F.K. Chan, G. Kroemer, Necroptosis: mechanisms and relevance to disease, Annu. Rev. Pathol. 12 (2017) 103–130.

[26] M. Overholtzer, A.A. Mailleux, G. Mouneimne, G. Normand, S.J. Schnitt, R. W. King, E.S. Cibas, J.S. Brugge, A nonapoptotic cell death process, entosis, that occurs by cell-in-cell invasion, Cell 131 (2007) 966–979.

[27] W.S. Yang, B.R. Stockwell, Ferroptosis: death by lipid peroxidation, Trends Cell Biol. 26 (2016) 165–176.

[28] N. Mizushima, M. Komatsu, Autophagy: renovation of cells and tissues, Cell 147 (2011) 728–741.

[29] J. Liu, F. Kuang, R. Kang, D. Tang, Alkaliptosis: a new weapon for cancer therapy, Cancer Gene Ther. 27 (2020) 267–269.

[30] H. Bian, S. Zhang, H. Wu, Y. Wang, Interpretation of immunohistochemistry data of tumor should consider microenvironmental factors, Tumour Biol. 36 (2015) 4467–4477.

[31] W. Chen, R. Zheng, S. Zhang, H. Zeng, C. Xia, T. Zuo, Z. Yang, X. Zou, J. He, Cancer incidence and mortality in China, 2013, Cancer Lett. 401 (2017) 63–71.

[32] M. Dankner, A.A.N. Rose, S. Rajkumar, P.M. Siegel, I.R. Watson, Classifying BRAF alterations in cancer: new rational therapeutic strategies for actionable mutations, Oncogene 37 (2018) 3183–3199.

[33] E.F. Giunta, V. De Falco, S. Napolitano, G. Argenziano, G. Brancaccio, E. Moscarella, D. Ciardiello, F. Ciardiello, T. Troiani, Optimal treatment strategy for metastatic melanoma patients harboring BRAF-V600 mutations, Ther. Adv. Med. Oncol. 12 (2020), 1758835920925219.

[34] A.M. Haugh, D.B. Johnson, Management of V600E and V600K BRAF-mutant melanoma, Curr. Treat. Options Oncol. 20 (2019) 81.

[35] P.M. LoRusso, K. Schalper, J. Sosman, Targeted therapy and immunotherapy: Emerging biomarkers in metastatic melanoma, Pigment Cell Melanoma Res. 33 (2020) 390–402.

[36] S.A. Weiss, J.D. Wolchok, M. Sznol, Immunotherapy of melanoma: facts and hopes, Clin. Cancer Res. 25 (2019) 5191–5201.

[37] S.S. Gnanendran, L.M. Turner, J.A. Miller, S.J.E. Hwang, A.C. Miller, Cutaneous adverse events of anti-PD-1 therapy and BRAF inhibitors, Curr. Treat. Options Oncol. 21 (2020) 29.

[38] J. de Haan, J.V. van Thienen, M. Casaer, R.A. Hannivoort, K. Van Calsteren, M. van Tuyl, M.M. van Gerwen, A. Debeer, F. Amant, R.C. Painter, Severe adverse reaction to vemurafenib in a pregnant woman with metastatic melanoma, Case Rep. Oncol. 11 (2018) 119–124.

[39] J. Liu, X. Chen, T. Ward, M. Pegram, K. Shen, Combined niclosamide with cisplatin inhibits epithelial-mesenchymal transition and tumor growth in cisplatin-resistant triple-negative breast cancer, Tumour Biol. 37 (2016) 9825–9835.

[40] Q. Luo, J.M. Beaver, Y. Liu, Z. Zhang, Dynamics of p53: a master decider of cell fate, Genes 8 (2017) (Basel).

[41] S.L. Harris, A.J. Levine, The p53 pathway: positive and negative feedback loops, Oncogene 24 (2005) 2899–2908.